Citation:

Gardi, A and Sabatini, R 2015, 'Bistatic measurement system for characterisation of aviation pollutant concentrations', in Arvind Sinha, Cees Bil, Bogdan Hristea, Bob Teunisse (ed.) Proceedings of the16th Australian International Aerospace Congress, Barton, Australia, 23-24 February 2015, pp. 1-18.

See this record in the RMIT Research Repository at:

https://researchbank.rmit.edu.au/view/rmit:30616

Version: Accepted Manuscript

Link to Published Version:

http://www.aiac16.com/index.php/program/call-for-submissions

Bistatic Measurement System for Characterisation of Aviation Pollutant Concentrations

Alessandro Gardi and Roberto Sabatini
School of Aerospace, Mechanical and Manufacturing Engineering, RMIT University
Melbourne, VIC 3000, Australia

Abstract

This paper presents the conceptual design of a low-cost measurement system for the determination of aviation-related pollutant concentrations in dense air traffic areas. The proposed bistatic Light Detection and Ranging (LIDAR) system consists of two non-collocated components. The source component consists of a tuneable laser emitter, which can either be installed on a Remotely Piloted Aircraft System (RPAS) or operated from fixed and movable surface installations. The sensor component is constituted by a target surface calibrated for reflectance and a rail-mounted visible or infrared camera calibrated for radiance. The system performs Differential Absorption LIDAR (DIAL) measurements. The relevant opportunities and challenges, and the viability of the system in the intended operational environments are discussed. Numerical simulation results show promising performances in term of error expected error budget even in degraded meteorological conditions, which are comparable to the more complex and relatively costly monostatic LIDAR techniques currently available.

Keywords: Aircraft Emissions, Differential Absorption, DIAL, LIDAR, Pollutant Measurement, Sustainable Aviation.

Introduction

Current research activities are addressing new sensor technologies and measurement techniques for the determination of aviation pollutant concentrations. The new systems should feature either: greater operational flexibility, better sensitivity, accuracy, precision, reliability, greater spectral/spatial/temporal resolutions, and reduced weight/volume/costs. The research community is interested, in particular, in the spatial and temporal variations of macroscopic observables, and on the microphysical and chemical properties of atmospheric constituents and pollutants, including molecular, aerosol and particulate species [1-3]. An accurate measurement of CO_2 concentration variations in space and time related to aircraft operations is particularly important. The advent of powerful LIDAR systems with low weight and packaged in relatively small casings, makes them well suited for measuring the column densities of various important molecular species, including carbon oxides (CO_X), nitrogen oxides (NO_X), sulphur oxides (SO_X), oxygen (O_2) and ozone (O_3), both locally and over extended geographic areas [4, 5]. The Near-Infrared (NIR) region of the atmospheric propagation spectrum is dominated by molecular absorption from H_2O, CO and CO_2. A comparison with recorded spectra enables the identification of relatively strong and isolated CO and CO_2 transitions for unambiguous species detection [6]. These transitions have formed the basis of NIR sensors for measurements of CO and CO_2 mole fractions in exhaust gases using extraction-sampling techniques and for non-intrusive measurements of CO_2 in high-temperature combustion environments. Based on the demonstrated potential of Differential Absorption LIDAR (DIAL) [7-9], new airborne DIAL systems will greatly benefit from the technological advances in tuneable, compact and low-cost laser emitters enabling further portions of the spectrum to be exploited for multi-species pollutant concentration measurements.

Bistatic DIAL Measurement System

The bistatic measurement system was conceptually presented in [10], based on previous research [2, 3, 11-15]. The proposed system is based on the DIAL technique [16]. The laser source emits beams at two predefined wavelengths. The first wavelength (λ_{ON}) is selected in correspondence of a major vibrational band of the targeted pollutant molecule (on-absorption line), clear from the transition/vibration spectrum of other atmospheric components. The second wavelength (λ_{OFF}) is selected in proximity of the first, but outside the vibrational band (off-absorption line) of the targeted pollutant species, so that the difference in cross-sections, $\Delta\psi \triangleq \psi(\lambda_{ON}) - \psi(\lambda_{OFF})$ is maximised. A number of databases and atmospheric Radiative Transfer Model (RTM) codes are available and allow an accurate estimation of the propagation spectrum for identifying the optimal combination of DIAL wavelengths based on the mentioned criteria. As depicted in Fig. 1, the proposed bistatic DIAL measurement system consists of a LIDAR emitter installed on a RPAS or on fixed/movable surface installations, and a sensor component. The sensor component consists of a target surface featuring high and diffused reflectance and exhibiting Lambertian behaviour, such as Spectralon™, and a visible/infrared camera mounted on a rail. The RPAS platform flies pre-determined trajectories based on the required space and time frames of the measurement. The functional block diagram of the bistatic DIAL measurement system is represented in Fig. 2.

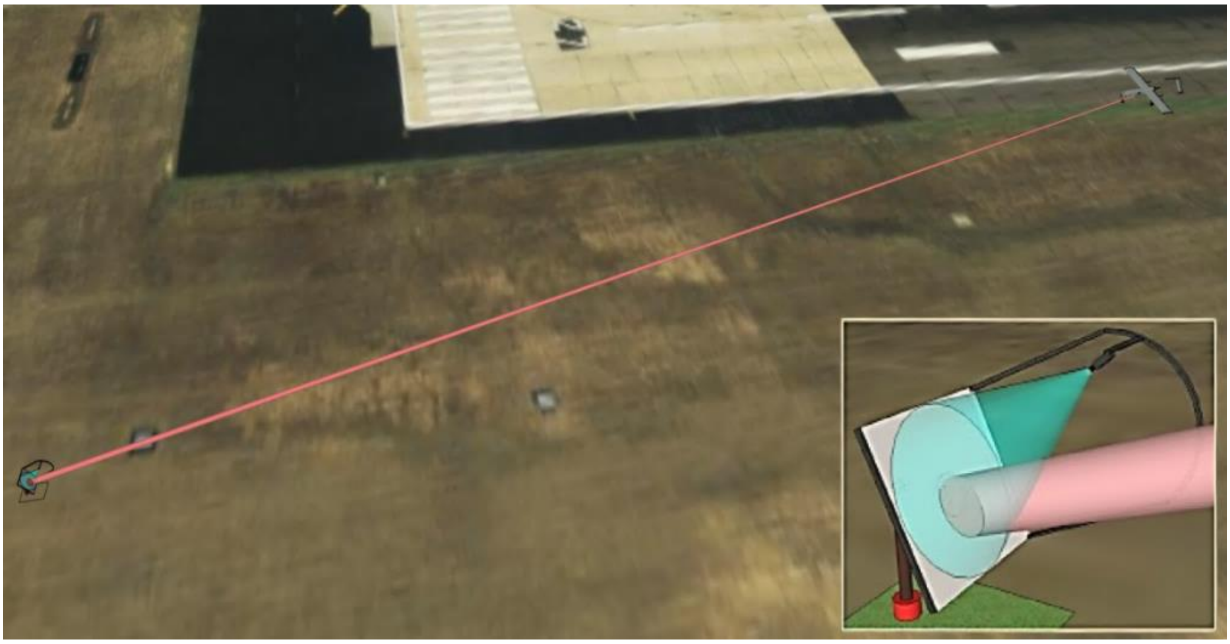

Fig. 1: Representation of the bistatic DIAL system, not to scale [17].

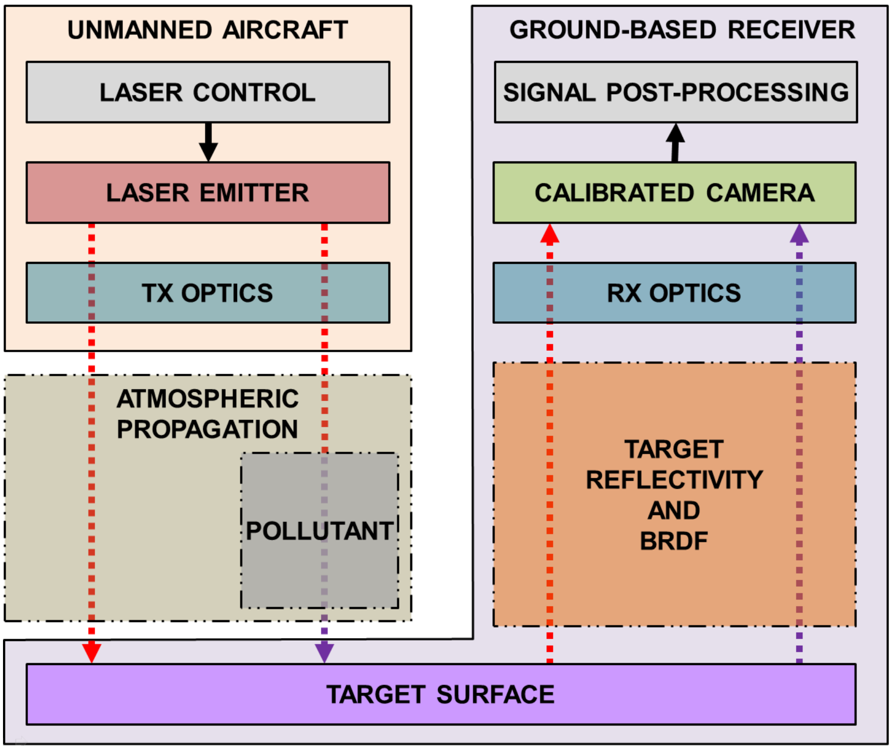

Fig. 2: Functional block diagram of the bistatic DIAL measurement system [18].

Atmospheric Laser Beam Propagation

The propagation of laser radiation in atmosphere is affected by a number of linear and nonlinear effects. In [17] we described the following expression for the peak irradiance I_P, accounting for absorption, scattering, diffraction, jitter, atmospheric turbulence and thermal blooming effects assuming a Gaussian profile of the laser beam at the source and an average focused irradiance [19, 20]:

$$I_P(z,\lambda) = \frac{b(z)\,\tau(z,\lambda)\,P(\lambda)}{\pi\left(a_d^2(z,\lambda) + a_j^2(z) + a_t^2(z,\lambda)\right)} \tag{1}$$

where z is the linear coordinate along the beam, λ is the wavelength, $P(\lambda)$ is the transmitted laser power, b is the blooming factor, $\tau(z,\lambda)$ is the transmittance coefficient, which accounts for absorption and scattering associated with all molecular and aerosol species present in the path. The 1/e beam radiuses associated with diffraction, $a_d(z,\lambda)$, beam jitter, $a_j(z)$, and turbulence, $a_t(z,\lambda)$, can be calculated as [3, 19]:

$$a_d(z,\lambda) = \frac{Qz\lambda}{2\pi a_0} \tag{2}$$

$$a_j^2(z) = 2\langle\Theta_x^2\rangle\, z^2 \tag{3}$$

$$a_t(z,\lambda) = \frac{2\, C_N^{6/5} z^{8/5}}{\lambda^{1/5}} \tag{4}$$

where Q is the beam quality factor, a_o is the beam *1/e* radius, $\langle\Theta_x^2\rangle$ is the variance of the single axis jitter angle that is assumed to be equal to $\langle\Theta_y^2\rangle$, and C_N^2 is the refractive index structure constant. An empirical model for the blooming factor $b(z)$, which is the ratio of the bloomed I_B to unbloomed I_{UB} peak irradiance, is:

$$b(z) = \frac{I_B}{I_{UB}} = \frac{1}{1 + 0.0625\, N^2(z)} \tag{5}$$

N is the thermal distortion parameter, calculated as:

$$N(z) = \frac{-n_T\, \alpha_m\, P\, z^2}{\pi\, d_0\, v_0\, c_P\, a_0^3} \cdot \left[\frac{2}{z^2}\int_0^R \frac{a_0}{a(z')}dz' \int_0^{z'} \frac{a_0^2\, v_0\, \tau''}{a}\, dz''\right] \tag{6}$$

where v_o is the uniform wind velocity in the weak attenuation limit ($\gamma z << 1$), n_T , d_o , and c_p are, respectively, the coefficients of index change with respect to temperature, density, and specific heat at constant pressure. The transmittance coefficient τ depends on the integral effect of absorption and scattering phenomena, both for molecular and aerosol species, on the entire beam length. The expression of Beer's law highlighting such dependences can therefore be written as:

$$\tau(z,\lambda) = e^{-\int_0^z \gamma(z,\lambda)\, dz} = e^{-\int_0^z [\alpha_m(z,\lambda) + \alpha_a(z,\lambda) + \beta_m(z,\lambda) + \beta_a(z,\lambda)]\, dz} \tag{7}$$

where α are the absorption coefficients and β are the scattering coefficients, the subscripts *m* and *a* refer respectively to molecular and aerosol contributions. When referring to the integral absorption and scattering due to specific molecular species, it is more appropriate to express the transmittance with the following model:

$$\tau(z,\lambda) = e^{-\int_0^z \gamma(z,\lambda)\, dz} = e^{-\int_0^z \sum_i [\psi_i(\lambda) \cdot n_i(z)]\, dz} \tag{8}$$

where:
$\psi_i(\lambda)$ = cross-section of the ith species
n_i = molecular volume density of the ith species
From Eq. 8, the fraction between the measured incident laser energy associated with the on-absorption line of pollutant species *P* and the one associated with the off-absorption line, $R_{ON/OFF}$, can be expressed as [10]:

$$R_{ON/OFF} = \frac{E(\lambda_{ON})}{E(\lambda_{OFF})} = \frac{\tau_{ON}}{\tau_{OFF}} = e^{-[\psi_P(\lambda_{ON}) - \psi_P(\lambda_{OFF})]\int_0^D n_P(r)\, dr} \tag{9}$$

where *D* is the total beam length. The total pollutant column density N_P, which is the integral of the molecular volume density on the entire beam, is therefore:

$$N_P = \int_0^D n_P(r)\, dr = \frac{-\ln(R_{ON/OFF})}{\Delta\psi} \tag{10}$$

The average molecular volume concentration of the pollutant on the path, $\tilde{n}_P$, is therefore:

$$\tilde{n}_P = \frac{N_P}{D} = \frac{-\ln(R_{ON/OFF})}{D \cdot \Delta\psi} \tag{11}$$

As evident from Eq. 9 to 11, the bistatic DIAL measurement system neglects most of the parasite phenomena such as atmospheric visibility, particulate, rain and other precipitations, which would have elsewhere introduced a number of additional uncertainties in the system. The parasite effects, in fact, are assumed to equally affect the off-absorption and the on-absorption transmittances.

Aerosol Retrieval

The retrieval of aerosol concentrations was originally examined in [2]. As per eq. 7, both molecular and aerosol concentrations in the transmission medium (i.e. the atmosphere) introduce absorption and scattering phenomena that affect the laser beam propagation. Therefore, the atmospheric transmittance measurement data accumulated in a certain time period using passive imaging systems enable the retrieval of aerosol concentrations as well. The difficulty in developing inversion algorithms lies in the fact that the input optical data are related to the investigated microphysical parameters through nonlinear integral equations of the first kind (Fredholm equations), which cannot be solved analytically. The generalised form of the Fredholm equation for atmospheric data retrieval is:

$$\alpha(\lambda), \beta(\lambda) = \int K_{\alpha,\beta}(r, n, k, \lambda) \cdot D(r) dr \quad (12)$$

where $\alpha(\lambda)$, and $\beta(\lambda)$ represent the optical data, $K_{\alpha,\beta}$ is the atmospheric kernel function (containing information on particle size, refractive index etc.) and $D(r)$ is the particle size distribution. The numerical solution of these equations leads to the so called ill-posed inverse problem. Such problems are characterised by a strong sensitivity of the solution space toward uncertainties of the input data, the non-uniqueness of the solution space, and the incompleteness of the solution space. In fact, the solution space may still be correct in a mathematical sense, but might not necessarily reflect the physical conditions. As the problem cannot be entirely defined by the measurements, a priori knowledge of the state vector is required in order to determine the most probable solution, with a probabilistic Bayesian approach. Let $\boldsymbol{y}$ be the measurement vector containing the measured radiances, and $\boldsymbol{x}$ be the concentration of a given constituent, then the general remote sensing equation can be written as follows [5]:

$$\boldsymbol{y} = f(\boldsymbol{x}, \boldsymbol{b}) + \boldsymbol{\epsilon} \quad (13)$$

where f represents the forward transfer function, $\boldsymbol{b}$ the other parameters affecting the measurement, and $\boldsymbol{\epsilon}$ the measurement noise. In the case of instruments measuring laser radiance, the vector $\boldsymbol{b}$ includes the target surface reflectance and radiance features (BRDF, reflectivity, emissivity and temperature), the variables describing the atmospheric state (vertical turbulence profile, temperature, water vapour and other atmospheric constituents, clouds, aerosols, etc.), and some characteristics of the measurement instruments (spectral response functions and resolution). The inverse problem consists in retrieving $\hat{\boldsymbol{x}}$, an estimate of the true state $\boldsymbol{x}$, from the measurement $\boldsymbol{y}$, and can be expressed as:

$$\hat{\boldsymbol{x}} = R\left(\boldsymbol{y}, \hat{\boldsymbol{b}}\right) = R\left(f(\boldsymbol{x}, \boldsymbol{b}) + \boldsymbol{\epsilon}, \hat{\boldsymbol{b}}\right) \quad (14)$$

where $\hat{\boldsymbol{b}}$ is an estimate of the non-retrieved parameters $\boldsymbol{b}$, and R is the inverse transfer function. This a priori information consists of an a priori state vector $\boldsymbol{x_a}$ and its covariance matrix $\boldsymbol{S_a}$, which may be provided by model simulations. Therefore, the inverse problem can be rewritten as follows:

$$\hat{\boldsymbol{x}} = R\left(\boldsymbol{y}, \hat{\boldsymbol{b}}, \boldsymbol{x_a}\right) \quad (15)$$

Various inversion techniques were proposed. One of the most popular approaches is the inversion with regularisation, offering the advantage of reducing oscillations in the solution that are frequently experienced in data retrieved from electro-optical measurements [1, 19]. This approach consists in introducing constraints, such as derivative analysis (smoothness) of the particle size distribution functions, positive sign of the functions and maximum variations over time. Using appropriate kernel/base functions, this algorithm can deliver parameters such as effective (average) particle radius, particle size distribution, total surface-area concentration, total number/volume concentrations, real and imaginary parts of the refractive index, single scattering albedo, etc. The base functions are Gaussian fits of the existing particle concentration data and are used to reconstruct the investigated particle size distributions. The kernel functions describe the interaction of laser radiation with the atmosphere and contain information about the atmospheric transmittance, including scattering and absorption processes.

Error Estimation

A preliminary error estimation was presented in [17]. The uncertainty associated with the measurement of the molecular volume concentration, derived from Eq. 11, is:

$$\sigma_{\tilde{n}_P} = \frac{1}{D \cdot \Delta\psi} \sqrt{\left(\frac{\sigma_{R_{ON/OFF}}}{R_{ON/OFF}}\right)^2 + \left(\frac{\sigma_D \ln R_{ON/OFF}}{D}\right)^2 + \left(\frac{\sigma_{\Delta\psi} \ln R_{ON/OFF}}{\Delta\psi}\right)^2} \qquad (16)$$

For a preliminary estimation, we introduced representative errors on the first two quadratic terms in eq. 16, specific to the bistatic DIAL implementation. Errors were introduced on the distance, σ_D, and on the differential energy measurement, which is translated into $\sigma_{R_{ON/OFF}}$ by means of the Bidirectional Reflectance Distribution Function (BRDF) of the target surface [3]. Assuming the operational conditions summarised in Table 1 and injecting source errors detailed in Table 2, the resulting relative error for the CO_2 volume density was calculated as $\frac{\sigma_{\tilde{n}_P}}{\tilde{n}_P}$ = 6.77 % [17].

Table 1: Assumed worst-case operative conditions [17].

Parameter	Value
Horizontal distance between the RPAS and the target surface	1000 m
RPAS Height Above Ground Level (AGL)	150 m
CO_2 volume density	300 ppm

Table 2: Assumed source errors [17].

Source	Magnitude	Affected Term	Error
Discrepancy in the incident angle between $E(\lambda_{ON})$ and $E(\lambda_{OFF})$	5° azimuth 5° elevation	$\frac{\sigma_{R_{ON/OFF}}}{R_{ON/OFF}}$	3.04 %
Degraded RPAS navigation performance	20 m horizontally 15 m vertically	$\frac{\sigma_D}{D}$	2.47%

These preliminary results, associated with the very low error figures from the monostatic Integral Path Differential Absorption (IPDA) LIDAR experimental campaigns [21] and with the estimated performance of the calibration technique proposed in [10], contribute to supporting the validity of the proposed bistatic DIAL measurement technique for high accuracy sensing of aviation-related pollutant concentrations. Experimental testing will be required to further corroborate these preliminary findings.

Conclusions and Future Work

This paper reviewed the recent research activities focussing on the development of an innovative bistatic LIDAR system for the measurement of pollutant concentrations. The specific implementations for carbon dioxide (CO_2) and aerosol measurements were presented. The Differential Absorption LIDAR (DIAL) technique allows neglecting parasite effects such as atmospheric visibility, particulate and precipitation, and contributes to the overall accuracy and reliability of the proposed technique. The uncertainty analysis for CO_2 column density measurements showed that the proposed technique produces satisfactory results even in degraded meteorological conditions, which are comparable to the more complex and relatively costly monostatic LIDAR techniques currently available. Current research activities are investigating the extension of the system to other families of aviation pollutants such as nitrogen oxides (NO_X), sulphur oxides (SO_X), and Volatile Organic Compounds (VOC) taking advantage of the recent availability of tuneable laser emitters for multi-species detection. The research activities will involve laboratory testing as well as flight testing in various representative conditions. In particular, the development of the airborne component will benefit from the concurrent research activities on RPAS-based LIDAR systems [22-24]. The RPAS will be equipped with Differential GPS-based Time-and-Space-Position-Information (TSPI) systems that were developed for augmented navigation performance of both manned and unmanned aircraft [25, 26] in combination with integrity augmentation systems [27-29]. The experimental flight testing activity will be performed in a suitably developed laser test range in full compliance with eye-safety requirements [3, 13, 30]. The full potential of the proposed bistatic DIAL measurement system will be exploited through its functional integration in the next generation of Air Traffic Management (ATM) systems [31-34].

References

1. Rodgers, C. D., *Inverse methods for atmospheric sounding: Theory and practice* vol. 2: World scientific Singapore, 2000.
2. Sabatini, R., Richardson, M. A., Jia, H., and Zammit-Mangion, D., "Airborne laser systems for atmospheric sounding in the near infrared", in proceedings of *SPIE 8433, Laser Sources and Applications, Photonics Europe 2012*, Brussels, Belgium, 2012. DOI: 10.1117/12.915718
3. Sabatini, R. and Richardson, M. A., *Airborne Laser Systems Testing and Analysis*: NATO Science and Technology Organization, 2010.
4. Veselovskii, I., Kolgotin, A., Griaznov, V., Müller, D., Franke, K., and Whiteman, D. N., "Inversion of multiwavelength Raman lidar data for retrieval of bimodal aerosol size distribution", *Applied Optics,* vol. 43, pp. 1180-1195, 2004. DOI: 10.1029/2003JD003538
5. Müller, D., Wagner, F., Wandinger, U., Ansmann, A., Wendisch, M., Althausen, D., *et al.*, "Microphysical particle parameters from extinction and backscatter lidar data by inversion with regularization: Experiment", *Applied Optics,* vol. 39, pp. 1879-1892, 2000
6. Kuang, Z., Margolis, J., Toon, G., Crisp, D., and Yung, Y., "Spaceborne measurements of atmospheric CO2 by high-resolution NIR spectrometry of reflected sunlight: An introductory study", *Geophysical Research Letters,* vol. 29, pp. 11-1, 2002
7. Grant, W. B. and Hake Jr, R. D., "Calibrated remote measurements of SO2 and O3 using atmospheric backscatter", *Journal of Applied Physics,* vol. 46, pp. 3019-3023, 1975. DOI: 10.1063/1.321992
8. Grant, W. B., Hake Jr, R. D., Liston, E. M., Robbins, R. C., and Proctor Jr, E. K., "Calibrated remote measurement of NO2 using the differential-absorption backscatter technique", *Applied Physics Letters,* vol. 24, pp. 550-552, 1974. DOI: 10.1063/1.1655049
9. Schotland, R. M., "Errors in the lidar measurement of atmospheric gases by differential absorption", *Journal of Applied Meteorology,* vol. 13, pp. 71-77, 1974
10. Gardi, A., Sabatini, R., and Wild, G., "Unmanned aircraft bistatic lidar for CO2 colum density determination", in proceedings of *IEEE Metrology for Aerospace (MetroAeroSpace 2014)*, Benevento, Italy, 2014. DOI: 10.1109/MetroAeroSpace.2014.6865892

11. Sabatini, R., "Tactical Laser Systems Performance Analysis in Various Weather Conditions", in *RTO-MP-001 - E-O Propagation, Signature and System Performance under Adverse Meteorological Conditions Considering Out of Area Operations*, pp. 29-1 to 29-13, NATO Research and Technology Organization (RTO), Naples, Italy, 1998.

12. Sabatini, R., Guercio, F., and Vignola, S., "Airborne laser systems performance analysis and mission planning", in *RTO-MP-046 - Advanced Mission Management and Systems Integration Technologies for Improved Tactical Operations*, NATO Research and Technology Organization (RTO), Florence, Italy, 1999.

13. Sabatini, R. and Richardson, M. A., "A new approach to eye-safety analysis for airborne laser systems flight test and training operations", *Optics and Laser Technology,* vol. 35, pp. 191-198, 2003. DOI: 10.1016/S0030-3992(02)00171-8

14. Sabatini, R. and Richardson, M. A., "Innovative methods for planetary atmospheric sounding by lasers", in proceedings of *AIAA Space 2008 Conference*, San Diego, CA, USA, 2008. DOI: 10.2514/6.2008-7670

15. Sabatini, R. and Richardson, M. A., "Airborne Laser Systems Testing, Safety Analysis, Modelling and Simulation", presented at the 21st Annual Symposium of the Society of Flight Test Engineers - European Chapter, Vergiate (VA), Italy, 2010.

16. Browell, E. V., Ismail, S., and Grant, W. B., "DIAL", in *Encyclopedia of Atmospheric Sciences*, 2003.

17. Gardi, A., Sabatini, R., and Ramasamy, S., "Bistatic LIDAR System for the Characterisation of Aviation-Related Pollutant Column Densities", *Applied Mechanics and Materials,* vol. 629, pp. 257-262, 2014. DOI: 10.4028/www.scientific.net/AMM.629.257

18. Gardi, A., Sabatini, R., and Wild, G., "Conceptual design of an unmanned aircraft laser system for aviation pollution measurements", in proceedings of *Practical Responses to Climate Change, Engineers Australia Convention 2014 (PRCC 2014)*, Melbourne, Australia, 2014. DOI: 10.13140/2.1.3707.5528

19. Gebhardt, F. G., "High Power Laser Propagation", *Applied Optics,* vol. 15, pp. 1479-1493, 1976

20. Sabatini, R. and Richardson, M. A., "Novel atmospheric extinction measurement techniques for aerospace laser system applications", *Infrared Physics and Technology,* vol. 56, pp. 30-50, 2013. DOI: 10.1016/j.infrared.2012.10.002

21. Abshire, J. B., Riris, H., Weaver, C. J., Mao, J., Allan, G. R., Hasselbrack, W. E., *et al.*, "Airborne measurements of CO2 column absorption and range using a pulsed direct-detection integrated path differential absorption lidar", *Applied Optics,* vol. 52, pp. 4446-4461, 2013. DOI: 10.1364/AO.52.004446

22. Sabatini, R., Gardi, A., and Richardson, M. A., "LIDAR Obstacle Warning and Avoidance System for Unmanned Aircraft", *International Journal of Mechanical, Aerospace, Industrial and Mechatronics Engineering,* vol. 8, pp. 62-73, 2014

23. Sabatini, R., Gardi, A., Ramasamy, S., and Richardson, M. A., "A Laser Obstacle Warning and Avoidance System for Manned and Unmanned Aircraft", in proceedings of *IEEE Metrology for Aerospace (MetroAeroSpace 2014)*, Benevento, Italy, 2014, pp. 616-621. DOI: 10.1109/MetroAeroSpace.2014.6865998

24. Sabatini, R., Gardi, A., and Ramasamy, S., "A Laser Obstacle Warning and Avoidance System for Unmanned Aircraft Sense-and-Avoid", *Applied Mechanics and Materials,* vol. 629, pp. 355-360, 2014. DOI: 10.4028/www.scientific.net/AMM.629.355

25. Sabatini, R., "High Precision DGPS and DGPS/INS Positioning for Flight Testing", in *RTO-MP-043 - 6th Saint Petersburg International Conference on Integrated Navigation Systems*, pp. 18-1 to 18-17, NATO Research and Technology Organization (RTO), Saint Petersburg, Russia, 1999.

26. Sabatini, R. and Palmerini, G. B., *Differential Global Positioning System (DGPS) for Flight Testing*: NATO Science and Technology Organization, 2008.

27. Sabatini, R., Moore, T., and Hill, C., "Avionics-based integrity augmentation system for mission- and safety-critical GNSS applications", in proceedings of *25th International Technical Meeting of the Satellite Division of the Institute of Navigation (ION GNSS 2012)*, Nashville, TN, 2012, pp. 743-763

28. Sabatini, R., Moore, T., and Hill, C., "A new avionics-based GNSS integrity augmentation system: Part 1 - Fundamentals", *Journal of Navigation,* vol. 66, pp. 363-384, 2013. DOI: 10.1017/S0373463313000027

29. Sabatini, R., Moore, T., and Hill, C., "A new avionics-based GNSS integrity augmentation system: Part 2 - Integrity flags", *Journal of Navigation,* vol. 66, pp. 501-522, 2013. DOI: 10.1017/S0373463313000143

30. Sabatini, R., "Innovative Flight Test Instrumentation and Techniques for Airborne Laser Systems Performance Analysis and Mission Effectiveness Evaluation", in proceedings of *IEEE Metrology for Aerospace (MetroAeroSpace 2014)*, Benevento, Italy, 2014, pp. 1-17. DOI: 10.1109/MetroAeroSpace.2014.6865886

31. Gardi, A., Sabatini, R., Ramasamy, S., and de Ridder, K., "4-Dimensional Trajectory Negotiation and Validation System for the Next Generation Air Traffic Management", in proceedings of *AIAA Guidance, Navigation, and Control Conference 2013 (GNC 2013)*, Boston, MA, USA, 2013. DOI: 10.2514/6.2013-4893

32. Gardi, A., Sabatini, R., Ramasamy, S., and Kistan, T., "Real-Time Trajectory Optimisation Models for Next Generation Air Traffic Management Systems", *Applied Mechanics and Materials,* vol. 629, pp. 327-332, 2014. DOI: 10.4028/www.scientific.net/AMM.629.327

33. Ramasamy, S., Sabatini, R., Gardi, A., and Liu, Y., "Novel flight management system for real-time 4-dimensional trajectory based operations", in proceedings of *AIAA Guidance, Navigation, and Control Conference 2013 (GNC 2013)*, Boston, MA, USA, 2013. DOI: 10.2514/6.2013-4763

34. Ramasamy, S., Sabatini, R., Gardi, A., and Kistan, T., "Next Generation Flight Management System for Real-Time Trajectory Based Operations", *Applied Mechanics and Materials,* vol. 629, pp. 344-349, 2014. DOI: 10.4028/www.scientific.net/AMM.629.344